Proton hole states in ^{95}Y and ^{95,97,99}Nb

E. R. Flynn and Ronald E. Brown
Los Alamos National Laboratory, Los Alamos, New Mexico 87545

F. Ajzenberg-Selove
University of Pennsylvania, Philadelphia, Pennsylvania 19104

J. A. Cizewski
Wright Nuclear Structure Laboratory, Yale University, New Haven, Connecticut 06511
(Received 8 February 1982)

The proton hole states of ^{95}Y and ^{95,97,99}Nb have been studied by the $(\vec{t},\alpha)$ reaction using a polarized beam of 17 MeV tritons on targets of ^{96}Zr and ^{96,98,100}Mo. The results yield a number of new levels as well as numerous new spin assignments based on the large analyzing powers characteristic of the $(\vec{t},\alpha)$ reaction. Examination of the systematics of the resulting level schemes indicates a tendency towards deformation with increasing neutron number, which is expected given the known deformed region above $A=100$. However, ^{97}Nb is also clearly affected by the $N=56$ subshell closure. This subshell closure has a major effect on the level structure of ^{96}Zr but is completely washed out in ^{98}Mo.

[NUCLEAR REACTIONS ^{96}Zr, ^{96,98,100}Mo$(\vec{t},\alpha)$, $E=17$ MeV; measured $\sigma(\theta)$, $A_y(\theta)$; deduced J^π. DWBA analysis.]

I. INTRODUCTION

There is substantial interest in the region around mass $A=100$, where a shape transition occurs for many elements as a function of increasing neutron number. The origin of this shape transition appears to be rather complex and involves an interaction between neutron and proton degrees of freedom; both quantities have a significant effect on where the shape transition occurs as well as on the rapidity of its onset. There now exist extensive experimental data in this region which indicate how this trend develops. The deformed characteristics of the neutron-rich isotopes were originally observed in the decay schemes of fission fragments,[1] with later more extensive measurements further mapping this deformed region.[2,3] Two neutron transfer measurements, which also probe neutron-rich nuclei, provided verification of these results and were used to examine the systematic trends of pairing excitations from spherical into deformed nuclei.[4–6] Thus, the evidence for this phase transition region is now well determined.

There have also been a number of theoretical attempts

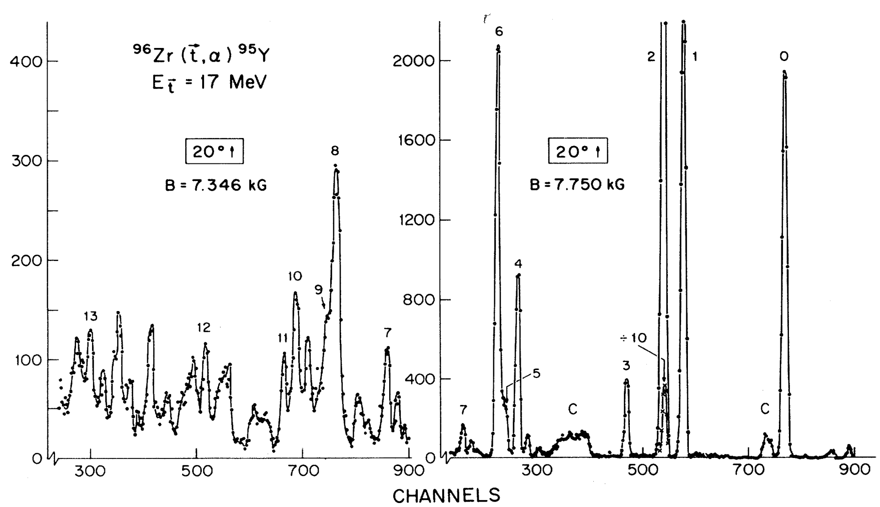

FIG. 1. ^{96}Zr$(\vec{t},\alpha)$ spectrum. The ordinate displays the number of counts in a two-channel bin.

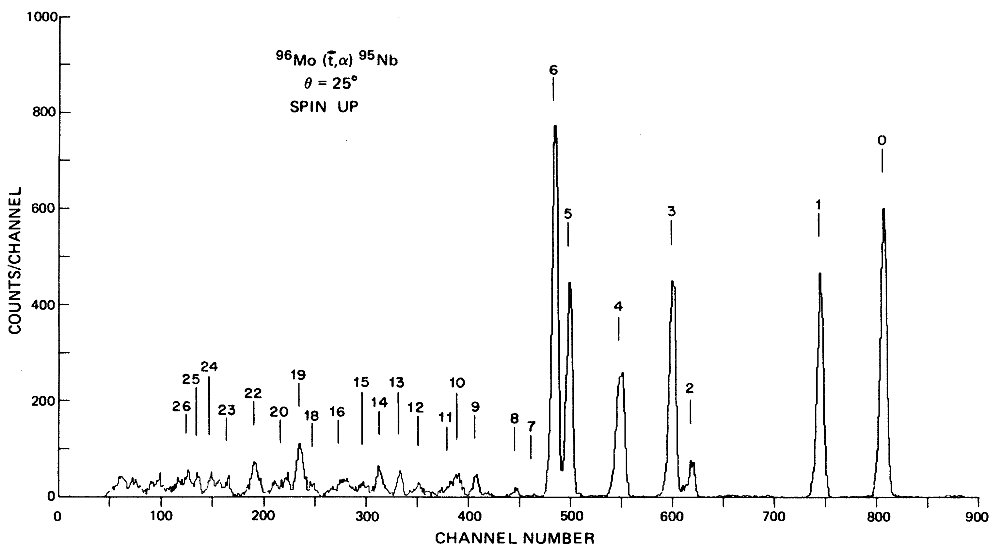

FIG. 2. ^{96}Mo($\vec{t}$,α) spectrum.

to explain the existence of this transition region. Recent work in this area has involved the interacting boson approximation[7] (IBA) model and consideration of the interaction between neutrons and protons as an important reason for the occurrence of deformation.[8] The importance of the role of the protons in the deformation-inducing process gives added impetus to an extensive study of the proton states in this region. There already exist some data regarding the proton hole excitations, based on earlier (d,^{3}He) and (^{3}He,d) reaction studies.[9–11] Recently, an investigation[12] of proton hole states in the nuclei ^{103}Tc and ^{109}Rh by ($\vec{t}$,α) reactions indicated a surprising anomaly. The resulting spectrum of ^{103}Tc showed a definite tendency towards deformation, with a strong shift in level structure compared to the surrounding odd proton nuclei as well as to the lighter Tc nuclei.[12] These results have lead to the present work, which is a systematic study of the Nb nuclei, with the purpose of looking for the mechanism responsible for the deformation tendency. The present results are in many ways similar to the previous (d,^{3}He) study,[9] but the analyzing power results (A_y) add significantly to the information and permit a large number of new J^π assignments.

II. EXPERIMENTAL TECHNIQUES

The experiments were conducted using a 17-MeV beam of tritons from the Los Alamos tandem Van de Graaff accelerator. The triton beam was polarized[13] with an average polarization of 0.78 and an average intensity of 45 nA. The reaction alpha particles were analyzed in a Q3D spectrometer with a solid angle of 14.3 msr and detected with a helical focal plane detector.[14] A solid state detector located at an angle of 30° monitored the elastic scattering in order to obtain absolute cross sections as well as to ensure correct relative cross sections from angle to angle. The energy bite encompassed by the 1 m long focal plane detector amounted to about 3 MeV for each of the targets.

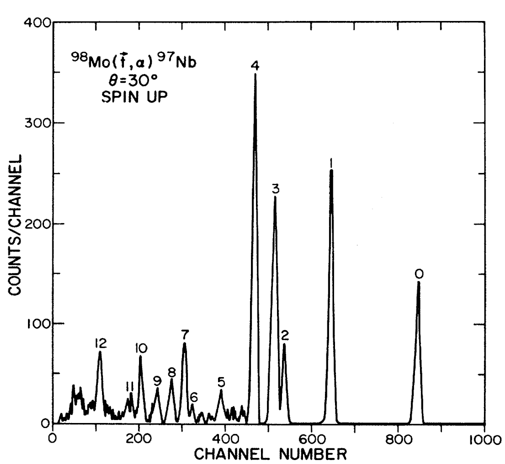

FIG. 3. ^{98}Mo($\vec{t}$,α) spectrum.

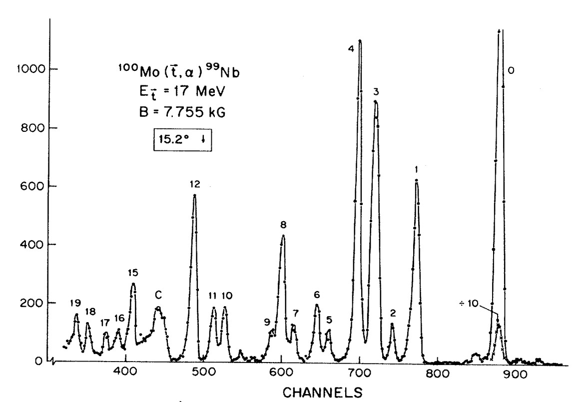

FIG. 4. ^{100}Mo($\vec{t}$,α) spectrum. The ordinate displays the number of counts in a two-channel bin.

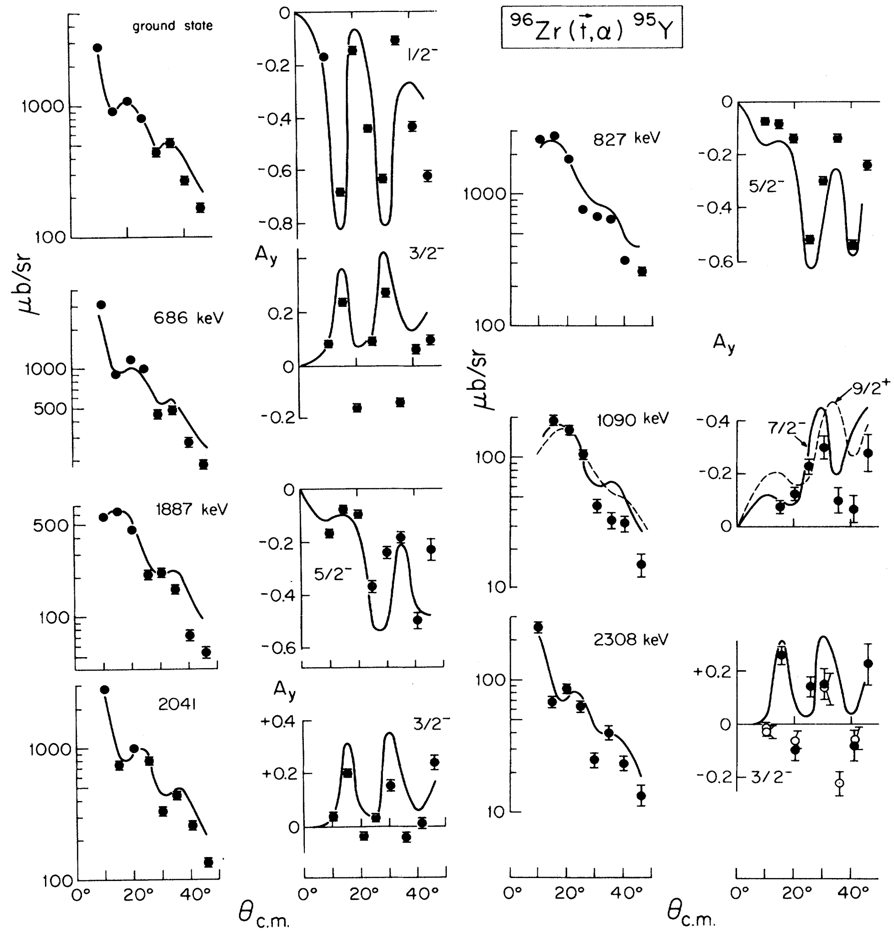

FIG. 5. Differential cross sections and A_y values for ^{95}Y.

All of the targets were rolled foils. The elastic scattering as measured by the monitor detector gave thicknesses for these foils which agreed with the weighed thicknesses to within ±10%. The thicknesses for the various targets were

$$^{96}\mathrm{Zr}=0.311\ \mathrm{mg/cm^2}\ ,$$

$$^{96}\mathrm{Mo}=0.218\ \mathrm{mg/cm^2}\ ,$$

$$^{98}\mathrm{Mo}=0.454\ \mathrm{mg/cm^2}\ ,$$

$$^{100}\mathrm{Mo}=0.194\ \mathrm{mg/cm^2}\ .$$

These target thicknesses dominated the energy resolution, about 24 keV FWHM for all targets except ^{98}Mo where the energy resolution was 36 keV.

Data were obtained at eight angles ranging from 10° to 45° in 5° steps. At each angle a spin up and spin down measurement was made with the spin being changed at the source. The polarization of the incident beam was measured in a computer controlled sequence at the beginning and end of each data taking run. The spectra were fitted on line and subsequently off line by the peak fitting program AUTOFIT to extract peak intensities and centroids. Energy calibrations were done either by using the ^{60}Ni(t,α) reaction whose Q values are well known or by using known levels[15] in the residual Nb nuclei.

III. RESULTS

Spectra for the ^{96}Zr and ^{96,98,100}Mo($\vec{t}$,α) reactions are shown in Figs. 1–4, respectively. The angular distributions and A_y values are displayed in Figs. 5–8. The energy levels are summarized in Tables I–IV. These tables contain our measured excitation energies and cross sections at 30° and give the J^π values which can be deduced from the shapes of the angular distributions of cross sections and A_y values when compared with distorted wave calculations (see below). Earlier results from (d,^{3}He) measurements[9,10] are also quoted.

Eight new levels are observed in ^{95}Y and twelve in ^{99}Nb. However, the principal new information in the present experiment is the definitive spin assignments. In the case of ^{95}Y no definite spin assignments had previously been made[15]; we are able to make seven J^π assignments. For ^{99}Nb the situation is similar: again no definitive spins had been known, but the J^π values of six levels are assigned here. One state of importance in ^{95}Y is the $\frac{9}{2}^+$ state at 1090 keV, which was not seen in the earlier (d,^{3}He) work,[10] although $\frac{9}{2}^+$ states were seen in the lighter Y nuclei. The observation of a $\frac{9}{2}^+$ state in ^{95}Y completes the wave function analysis made in Ref. 11 in which the mixture of $(1g_{9/2})^2$ and $(2p_{1/2})^2$ configurations in the Zr ground states was calculated.

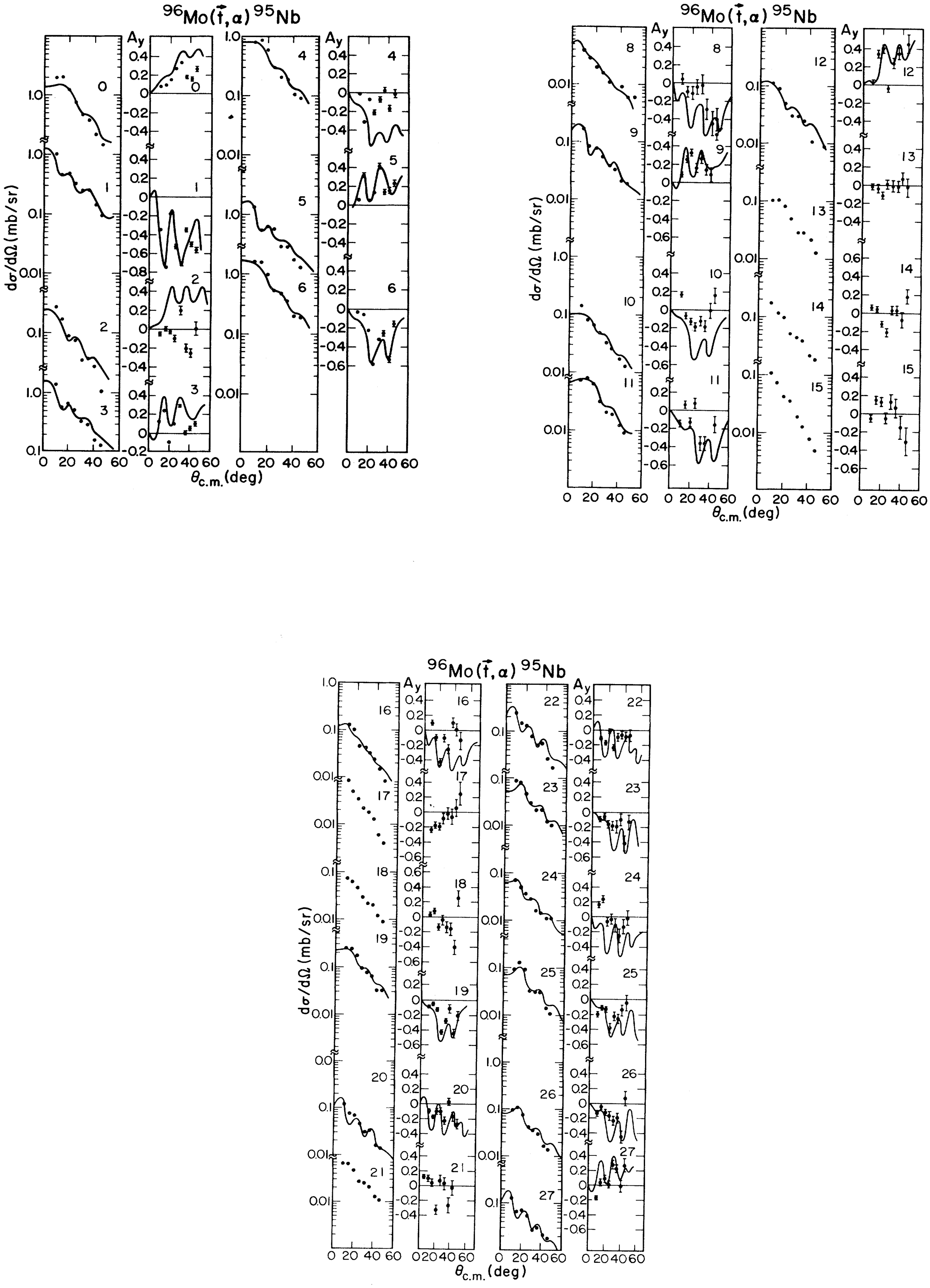

FIG. 6. Differential cross sections and A_y values for ^{95}Nb.

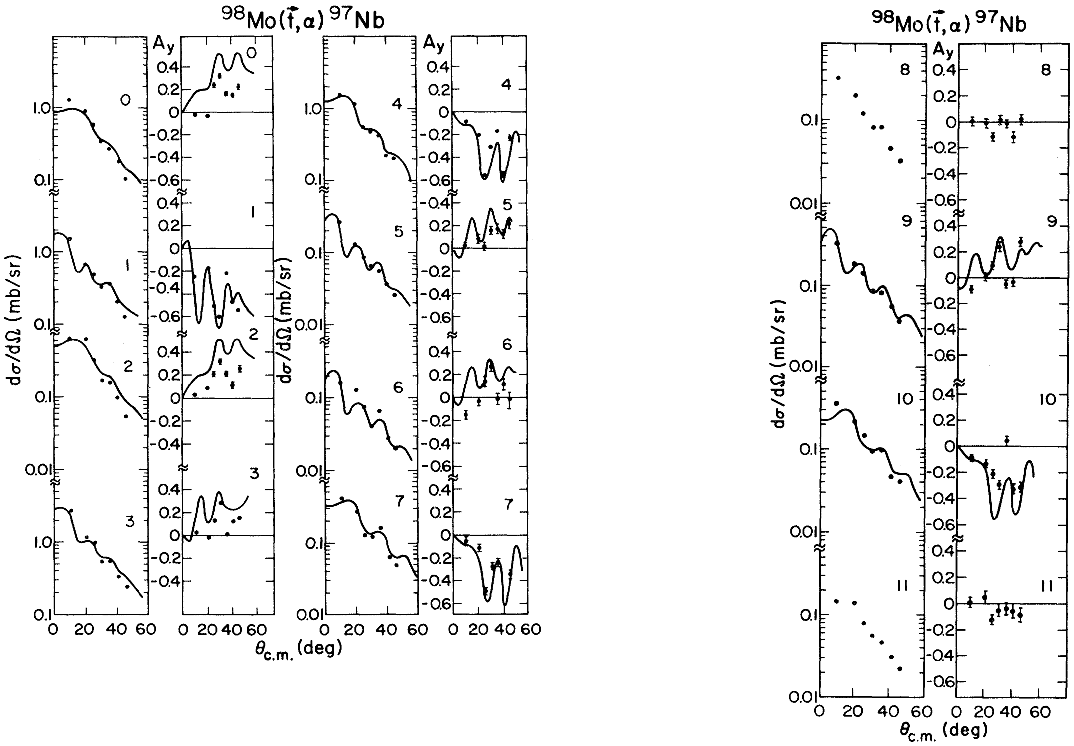

FIG. 7. Differential cross sections and A_y values for ^{97}Nb.

The calibration procedures mentioned above permitted the measurement of the ground state masses for the residual nuclei. In the case of ^{95}Y, the adopted mass excess in the literature[16] is $-81\,237\pm20$ keV. The present Q value of 8294 ± 20 keV leads to a mass excess of $-81\,214\pm20$ keV. For ^{99}Nb, the measured Q value of 8642 ± 20 keV gives a mass excess of $-82\,306\pm20$ keV, whereas the value quoted in Ref. 16 is $-82\,346\pm16$ keV. The masses for ^{97,95}Nb are well established, and the present Q values of $10\,019\pm20$ and $10\,524\pm20$ keV, respectively, agree to within 2 and 6 keV with the corresponding published values.

IV. DISTORTED WAVE CALCULATIONS

Distorted wave calculations (DW) were carried out using the code DWUCK.[17] The optical model parameters were obtained from surveys of elastic scattering of tritons[18] and alphas.[19] The parameters used are given in Table V. The calculated angular distributions of cross sections and analyzing powers are shown in Figs. 5–8.

The normalization used in DW calculations for the (t,α) reaction is always a problem, with values between 10 and 50 being reported.[21,22] In the present case, a sensitivity of the normalization constant to the optical model parameters was also observed. To circumvent this difficulty, the constant was chosen in order to give the expected total number of particles outside of the closed shell at $Z=28$, i.e., 14 particles for the case of Mo. A sum rule was used for this analysis. Similarly, for the Zr results 12 particles were required. In addition, the data reported in Ref. 12 were also considered in order to establish a consistent sum rule. In the relation

$$d\sigma/d\Omega=N(C^2S)d\sigma_{\rm DW}/(2J+1)\ ,$$

the value obtained from this analysis was $N=11.6$. This value yields 15.4 particles for ^{98}Mo and 11.5 particles for ^{96}Zr. The DW calculations were then done at 1 MeV intervals (in E_x) for all of the targets considered here. Since the principal goal of the present experiments was to establish the systematic trend of levels through a transitional region, the absolute normalization was not critical, although the sensitivity to the optical potential parameters would be of importance to reaction theories.

V. DISCUSSION

In the simple shell model, Zr fills the $f_{5/2}$, $p_{3/2}$, and $p_{1/2}$ proton orbitals with the $g_{9/2}$ orbital beginning to fill at Mo. There is, thus, a subshell closure occurring at Zr, although experimentally it is known that this is only partially true. Previous (d,^{3}He) results on the lighter Zr nuclei have shown evidence for $\frac{9}{2}^+$ strength present in the Zr ground states,[15] as the present results indicate for ^{96}Zr. The neutron number affects this proton strength, and it is this neutron-proton interaction which appears to cause the eventual onset of a shape deformation as both $g_{9/2}$ protons and $g_{7/2}$ neutrons are added.[8] A number of new spins in

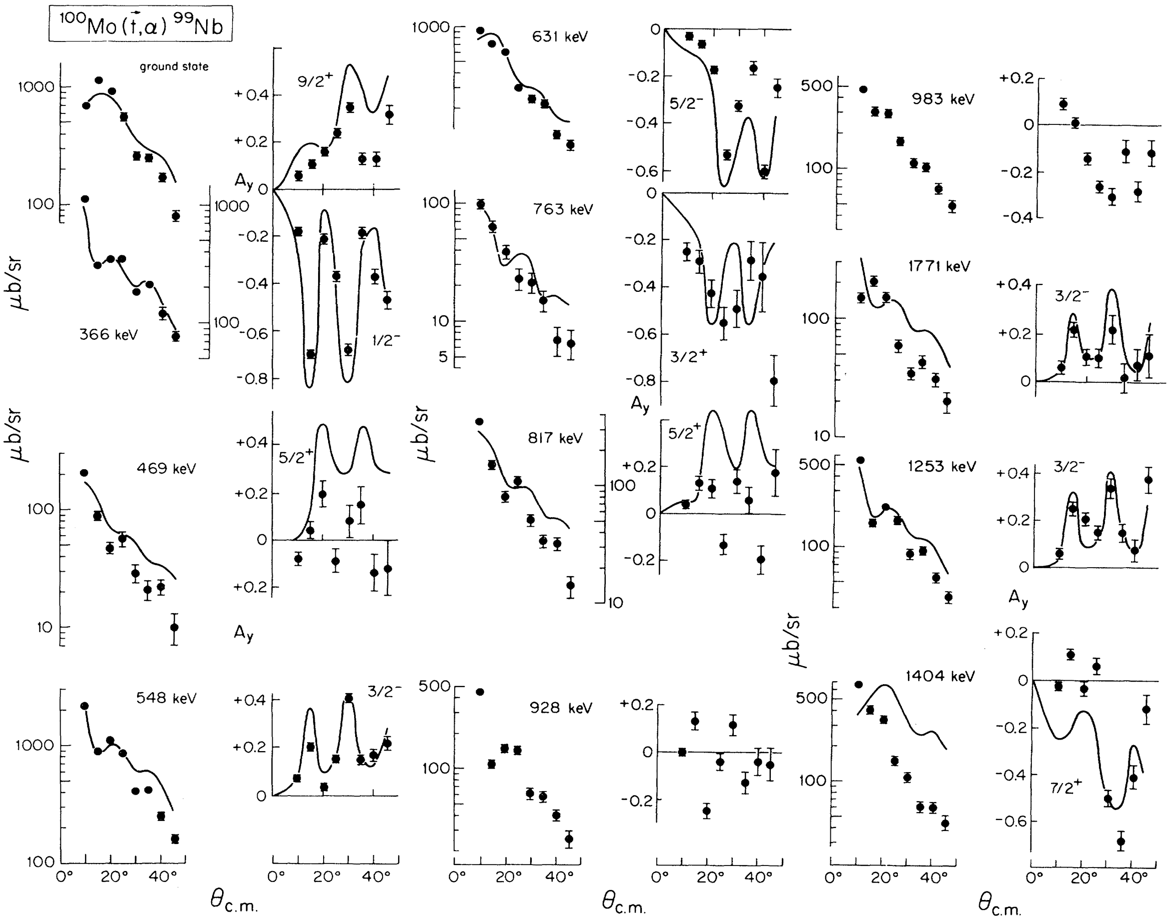

FIG. 8. Differential cross sections and A_y values for ^{99}Nb.

this work are assigned, thus creating a definitive set of levels to which such a theoretical analysis may be compared.

The analysis of ^{95}Y with the help of the A_y values confirms the spin assignments suggested by Preedom *et al.*[10] In Ref. 10, the $\frac{9}{2}^+$ state was not seen, and the ground state configuration mixing could only be estimated using the assumed $\frac{1}{2}^-$ strength in the ground state configuration. The present data shown in Table I make these assignments definite and also identify a candidate for the $\frac{9}{2}^+$ state at 1090 keV. Using the spectroscopic factors of Table I and normalizing the sum of $\frac{1}{2}^-$ and assumed $\frac{9}{2}^+$ state spectroscopic factors to the value of 2.0, we can assign the ^{96}Zr ground state coefficients to be 0.86 and 0.14 for the $p_{1/2}$ and $g_{9/2}$ configurations, respectively. These numbers turn out to be exactly those assumed by Preedom *et al.*[10] The spectroscopic values given in Table I agree well with those of Ref. 10 in a relative sense, but disagree by an overall normalization factor of 0.68 in absolute value.

Although the spectroscopic strengths of the low-lying $\frac{3}{2}^-$ and $\frac{5}{2}^-$ states agree quite well with simple shell model predictions, the structure of these states is more complicated. These states are also part of the particle vibration multiplets which arise from coupling the single-particle configurations to the 2_1^+ state of the even core nucleus. This character of the Y isotopes was identified in the ^{89}Y(t,p) measurements[20] and also characterizes some of the excitations in the Nb nuclei.

In Fig. 9 we show the level diagrams for the three Nb isotopes examined here. Two distinct features emerge from this figure. First, there is the more open level scheme of ^{97}Nb and the decreased level density associated with this. Second, ^{99}Nb illustrates a considerably compressed spectrum, possibly indicating a tendency towards deformation. This tendency was even more noticeable in the Tc isotopes, where ^{103}Tc showed substantial indication of deformation.[12]

The nucleus ^{97}Nb contains 56 neutrons. In the (t,p) reaction study of the Zr isotopes[21] it was noted that this neutron number, which closes the $d_{5/2}$ shell, had a substantial effect on the Zr level spacings as well as on the two nucleon transfer amplitudes, especially in the case of excited 0^+ states. All indications were that $N=56$ was a good subshell closure. On the other hand, similar (t,p) studies on the Mo isotopes showed almost no effect of this closure, and the systematics of both level schemes and transfer amplitudes are quite smooth through this region.[5] The present results indicate that the neutron subshell closure does indeed affect the Nb systematics. Thus, to some degree, ^{97}Nb looks more like a proton particle outside of

TABLE I. Results of ^{96}Zr($\vec{t}$,α)^{95}Y reaction measurements.

	Present work				Earlier measurements[a]		
Group no.[b]	E_x (MeV±keV)	$\sigma(30°)$ (mb/sr)	J^π	C^2S	E_x (MeV)	J^π	C^2S[g]
0	0[c]	0.45	$\frac{1}{2}^-$	2.7	0	$(\frac{1}{2})^-$	2.1
1	0.686±5	0.45	$\frac{3}{2}^-$	2.4	0.686	$\frac{3}{2},\frac{1}{2}^-$	1.9
2	0.827±5	0.65	$\frac{5}{2}^-$	9.9	0.827	$(\frac{5}{2})^-$	6.2
3	1.090±8	0.042	$\frac{7}{2}^-,\frac{9}{2}^+$				
	d				1.631		
4	1.887±8	0.21	$\frac{5}{2}^-$	2.5	1.88	$(\frac{5}{2})^-$	1.5
5	1.983±20				1.964		
6	2.041±10	0.33	$\frac{3}{2}^-$	2.2	2.047	$\frac{1}{2}^-,\frac{3}{2}^-$	1.4
7	2.308±10[e]	0.025	$\frac{3}{2}^-$	0.19			
8	2.603±10[e]						
9	2.655±20[e]						
					2.717		
					2.781		
10	2.855±20[e]						
11	2.906±20[f]				2.933		
					3.353		
12	3.405±20						
13	4.150±30						

[a]See Ref. 15.
[b]See Fig. 1.
[c]$Q_0 = 8294 \pm 20$ keV, as measured in this experiment; Q_m derived from the Wapstra-Bos masses (Ref. 16) is 8313±20 keV.
[d]This state is not observed; the intensity of groups corresponding to it are <5 percent of the intensity of the groups to ^{95}Y* (1.96).
[e]This group is too broad to be due to a single state.
[f]Above this group we are reporting the only two groups which are fairly sharp and which appear consistently at all angles. The density of states is too high above $E_x = 2.9$ MeV to permit identification of the states.
[g]See Ref. 10.

TABLE II. Results of ^{96}Mo($\vec{t}$,α)^{95}Nb reaction measurements.

	Present work				Earlier measurements[a]		
Group no.[b]	E_x (MeV±keV)	$\sigma(30°)$ (mb/sr)	J^π	C^2S	E_x (MeV)	J^π	C^2S
0	0[c]	0.47	$\frac{9}{2}^+$	2.9	0	$\frac{9}{2}^+$	2.54
1	0.237±8	0.25	$\frac{1}{2}^-$	1.7	0.236	$\frac{1}{2}^-$	1.50
2	0.732±8	0.035	$(\frac{5}{2})^+$	0.50	0.728[d]	$\frac{3}{2}^+,\frac{5}{2}^+$	
3	0.807±8	0.34	$\frac{3}{2}^-$	1.8	0.799	$\frac{3}{2}^-,\frac{5}{2}^-$	1.74
					0.92		
4	1.021±8	0.21	$(\frac{5}{2}^-)$	(2.6)	1.00	$\frac{5}{2}^-,\frac{7}{2}^-$	1.98
					1.09		
5	1.215±8	0.29	$\frac{3}{2}^-$	1.8	1.223	$\frac{1}{2}^-,\frac{3}{2}^-$	1.72
6	1.273±8	0.49	$\frac{5}{2}^-$	4.4	1.274	$\frac{1}{2}^-,\frac{3}{2}^-$	
7	1.364±8						
8	1.430±15[e]	0.011	$(\frac{3}{2}^+)$	(0.03)	1.412		

TABLE II. (*Continued.*)

	Present work				Earlier measurements[a]		
Group no.[b]	E_x (MeV±keV)	$\sigma(30°)$ (mb/sr)	J^π	C^2S	E_x (MeV)	J^π	C^2S
					1.514		
9	1.589±8	0.039	$\frac{3}{2}^-$	0.16	1.590	$\frac{3}{2}^+,\frac{5}{2}^+$	
10	1.662±8	0.033	$(\frac{5}{2}^-)$	(0.38)	1.632	$\frac{3}{2}^-+\frac{5}{2}^+$	0.14+0.06
11	1.701±8	0.020	$(\frac{7}{2}^+)$	(0.32)	1.691		
12	1.816±8	0.030	$\frac{5}{2}^+$	0.25	1.810	$\frac{3}{2}^+,\frac{5}{2}^+$	
13	1.894±8[d]	0.030			1.913	$\frac{3}{2}^+,\frac{5}{2}^+$	
14	1.972±8	0.045			1.970	$\frac{3}{2}^-+\frac{5}{2}^-$	0.07+0.6
15	2.045±8	0.020			2.070	$\frac{3}{2}^+,\frac{5}{2}^+$	
					2.121	$\frac{3}{2}^+,\frac{5}{2}^+$	
16	2.149±8	0.035			2.165	$\frac{3}{2}^+,\frac{5}{2}^+$	
17	2.180±8	0.018					
18	2.247±8	0.021	$(\frac{3}{2}^+,\frac{5}{2}^-)$		2.260		
19	2.302±8	0.080	$\frac{5}{2}^-$	0.82	2.328		
20	2.383±8	0.030	$\frac{1}{2}^-$	0.13	2.373		
21	2.421±8	0.025	$(\frac{3}{2}^+)$	(0.09)	{2.406, 2.431}		
22	2.486±8	0.050	$\frac{1}{2}^-$	0.27	2.48	$\frac{5}{2}^-,\frac{7}{2}^-$	1.17
23	2.599±8	0.020	$\frac{5}{2}^-$	0.31			
24	2.632±8	0.015	$(\frac{3}{2}^+)$	0.10	2.66		
25	2.670±8	0.030	$(\frac{5}{2}^-)$	0.42			
26	2.724±8	0.035	$\frac{5}{2}^-$	0.47			
27	2.768±8	0.028	$\frac{3}{2}^-$	0.12	2.79	$\frac{5}{2}^-,\frac{7}{2}^-$	1.12
28	2.815±8[f]				2.821		
29	2.896±8						
30	2.987±8				2.967	$\frac{3}{2}^+,\frac{5}{2}^+$	
31	3.039±8						

[a]See Refs. 15 and 9.
[b]See Fig. 2.
[c]Q_0=10 524±20 keV, as measured in this experiment; Q_m derived from the Wapstra-Bos masses (Ref. 16) is 10 516±4 keV.
[d]This group is too broad to be due to a single state.
[e]Two states.
[f]This state, and the three states below, were only observed at forward angles.

TABLE III. Results of ^{98}Mo($\vec{t}$,α)^{97}Nb reaction measurements.

	Present work				Earlier measurements[a]		
Group no.[b]	E_x (MeV)	$\sigma(30°)$ (mb/sr)	J^π	C^2S	E_x (MeV)	J^π	C^2S
0	0[c]	0.35	$\frac{9}{2}^+$	2.2	0	$\frac{9}{2}^+$	2.3
1	0.737±10	0.33	$\frac{1}{2}^-$	2.1	0.746	$\frac{1}{2}^-$	2.1
2	1.160±10	0.17	$\frac{9}{2}^+$	1.2	1.148		
3	1.247±10	0.54	$\frac{3}{2}^-$	2.6	1.251	$(\frac{3}{2})^-$	2.4
					1.276	$(\frac{5}{2})^+$	

TABLE III. (*Continued.*)

	Present work				Earlier measurements[a]		
Group no.[b]	E_x (MeV)	$\sigma(30°)$ (mb/sr)	J^π	C^2S	E_x (MeV)	J^π	C^2S
4	1.435±10	0.48	$\frac{5}{2}^-$	5.2	1.434	$(\frac{5}{2})^-$	(5.8)
					1.548	$(\frac{1}{2},\frac{3}{2}^-)$	
					1.653		
5	1.761±10	0.067[d]	$(\frac{3}{2}^-)$	(0.24)	1.754	$(\frac{5}{2})^+$	
					1.776	$(\frac{3}{2}^-)$	
					1.852	$(\frac{5}{2})^+$	
					1.945	$(\frac{7}{2}^+,\frac{9}{2}^+)$	
6	2.047±10	0.041	$(\frac{3}{2}^-)$	(0.07)	2.048	$(\frac{1}{2}^-,\frac{3}{2}^-)$	
					2.092		
					2.106	$(\frac{1}{2})^+$	
7	2.113±10	0.12	$\frac{5}{2}^-$	1.2			
					2.114	$(\frac{3}{2}^+,\frac{5}{2}^+)$	
8	2.241±10	0.081[e]			2.24	$(\frac{3}{2})^-$	(0.26)
					2.357	$(\frac{1}{2}^+)$	
9	2.388±10	0.085	$(\frac{3}{2}^-)$	(0.34)	2.39	$(\frac{3}{2}^-)$	(0.29)
					2.525	$\frac{3}{2}^+,\frac{5}{2}^+$	
10	2.541±10	0.095	$(\frac{5}{2}^-)$	(1.0)	2.55	$(\frac{3}{2})^-$	(0.37)
11	2.654±10	0.056[e]					
					2.676	$\frac{3}{2}^+,\frac{5}{2}^+$	
					2.69	$(\frac{1}{2}^-,\frac{3}{2}^-)$	
					2.702	$\frac{3}{2}^+,\frac{5}{2}^+$	
					2.727	$\frac{3}{2}^+,\frac{5}{2}^+$	
					2.748		
					2.792	$(\frac{1}{2}^+)$	
12	2.961±10	0.139[e]			2.95		
					2.981	$(\frac{1}{2}^+)$	

[a]See Refs. 15 and 9.
[b]See Fig. 3.
[c]$Q_0=10\,019\pm20$ keV, as measured in this experiment; Q_m derived from the Wapstra-Bos masses (Ref. 16) is $10\,021\pm4$ keV.
[d]This group may be due to unresolved states.
[e]This group is due to unresolved states.

TABLE IV. Results of ^{100}Mo($\vec{t},\alpha$)^{99}Nb reaction measurements.

	Present work				Earlier measurements[a]		
Group no.[b]	E_x (MeV)	$\sigma(30°)$ (mb/sr)	J^π	C^2S	E_x (MeV)	J^π	C^2S[e]
0	0[c]	0.26	$\frac{9}{2}^+$	2.6	0	$(\frac{9}{2})^+$	(2.6)
1	0.366±5	0.18	$\frac{1}{2}^-$	1.0	0.365	$(\frac{1}{2})^-$	(1.6)
					0.387	$(\frac{7}{2}^+)$	
2	0.469±5	0.29	$(\frac{5}{2}^+)$	(2.9)	0.469	$(\frac{5}{2}^+)$	
					0.498		

TABLE IV. (*Continued.*)

	Present work				Earlier measurements[a]		
Group no.[b]	E_x (MeV)	$\sigma(30°)$ (mb/sr)	J^π	C^2S	E_x (MeV)	J^π	C^2S[e]
3	0.548±8	0.41	$\frac{3}{2}^-$	2.7	0.544		(2.5)
4	0.631±8	0.24	$\frac{5}{2}^-$	3.4			
5	0.763±8	0.022	$\frac{3}{2}^+$	0.06			
6	0.817±8	0.050	$(\frac{5}{2}^+)$	(0.5)	0.82	$(\frac{5}{2}^+)$	(0.16)
7	0.928±10	0.063					
					0.959	$(\frac{1}{2}^+,\frac{3}{2}^+)$	
8	0.983±10[d]	0.12					
					1.015	$(\frac{3}{2}^+)$	
9	1.031±12	0.023					
10	1.253±12	0.087	$\frac{3}{2}^-$	0.52	1.27	$(\frac{3}{2}^-)$	(0.56)
11	1.305±12	0.043					
12	1.404±12	0.11	$(\frac{7}{2}^+)$	(3.2)	1.41	$(\frac{5}{2})^-$	(2.3)
13	1.543±12	0.016					
					1.57	$(\frac{5}{2})^-$	(1.0)
14	1.584±12	0.027					
15	1.703±15	0.035					
					1.75	$(\frac{1}{2}^-,\frac{3}{2}^-)$	(0.27)
16	1.771±15[d]	0.038	$(\frac{3}{2}^-)$	(0.39)			
17	1.831±20	0.017					
18	1.921±20	0.033					
					1.97	$(\frac{3}{2}^-)$	(0.27)
19	1.982±20	0.039					

[a]See Ref. 15.
[b]See Fig. 4.
[c]$Q_0=8642\pm20$ keV, as measured in this experiment; Q_m derived from the Wapstra-Bos masses (Ref. 16) is 8682±18 keV.
[d]This group is too broad to be due to a single state.
[e]Reference 9.

^{96}Zr than a proton hole outside of the ^{98}Mo core.

However, the Nb isotopes can also be understood quite well by considering the low-lying excitations as arising from the coupling of shell model configurations to the even-even molybdenum cores, an approach taken by Bindal and co-workers in Ref. 9. In their model they considered the coupling of the $g_{9/2}$, $f_{5/2}$, $p_{3/2}$, and $p_{1/2}$ quasiparticle orbitals to the ground and 2_1^+ states of the Mo nuclei; a quadrupole particle-core interaction was included. The existing (d,^{3}He) measurements were seen to be in reasonable agreement with their calculations. However, because our present measurements have allowed more de-

TABLE V. Optical model parameters used in the (t,α) DW calculations.

	V (MeV)	r_r (fm)	a_r (fm)	W (MeV)	r_i (fm)	a_i (fm)	Ref.
t	152	1.24	0.685	23	1.432	0.870	18
α	186	1.396	0.562	26	1.396	0.562	19
	$V_{s.o.}$ (MeV)	$r_{s.o.}$ (fm)	$a_{s.o.}$ (fm)				Ref.
	6.0	1.10	0.83				18

finite spin assignments, and, hence, some of the earlier experimental evidence has been superseded, we present an updated comparison between experiment and theory of the ground states and low-spin, negative-parity states in ^{95,97,99}Nb in Fig. 10.

In the picture of Bindal *et al.*,[9] the $\frac{9}{2}^+$ ground states are predominately due to coupling the $g_{9/2}$ orbital to the Mo ground states. Since the theoretical predictions for spectroscopic strengths are in excellent agreement with the empirical strengths, this treatment seems quite good. The $\frac{1}{2}^-_1$ and $\frac{3}{2}^-_1$ states in this model arise predominately from coupling the $p_{1/2}$ and $p_{3/2}$ orbitals to the Mo ground state. The model also does a good job of predicting both the excitation energies and spectroscopic strengths for these states.

The $\frac{5}{2}^-_1$ state in this model arises predominately from the coupling $p_{1/2}\otimes 2_1^+$; the $\frac{5}{2}^-_2$ and $\frac{5}{2}^-_3$ states have essentially equal amplitudes for $f_{5/2}$ and the coupled $p_{3/2}\otimes 2_1^+$ configurations. Therefore, the $\frac{5}{2}^-_1$ state is expected to receive relatively little spectroscopic strength, with the $\frac{5}{2}^-_2$ and $\frac{5}{2}^-_3$ states receiving most of the strength. The empirical evidence is quite different. The $\frac{5}{2}^-_1$ states in ^{95,97,99}Nb are quite strongly populated in the (t,α) reaction and tend to be observed lower in excitation than the model would predict, especially in ^{99}Nb. The data may be indicating that the $f_{5/2}$ quasiparticle orbital lies lower in the spectrum than the work of Bindal *et al.*[9] expected, so that the $\frac{5}{2}^-_1$ state has a larger $f_{5/2}$ component, reflected in the observed strength. Higher in the spectra of $^{95-99}$Nb numerous negative-parity states and unassigned states are observed, and the earlier calculations[9] predict numerous fragments of the single-particle orbitals and resultant couplings to the 2_1^+ states of the cores in this energy region.

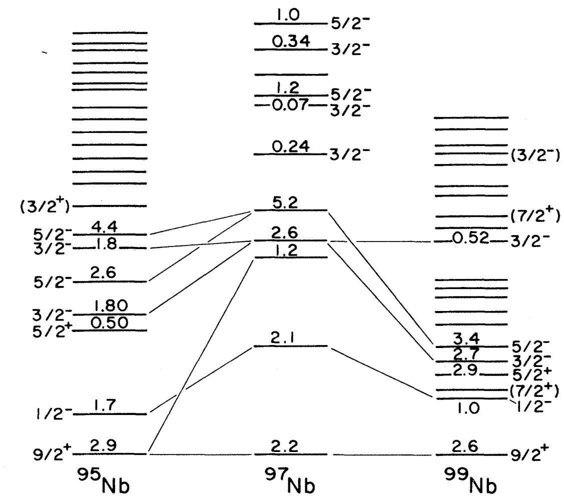

FIG. 9. Systematics of low lying levels in Nb isotopes. Numbers above lines are (t,α) spectroscopic factors.

The calculations for positive-parity states were only done for ^{99}Nb in the work of Ref. 9. We see considerably more positive-parity strength in these nuclei than their model would predict. In particular, $\frac{5}{2}^+$ states are seen in ^{95,99}Nb quite low in the spectra, while Bindal *et al.* predict the $\frac{5}{2}^+_1$ state at 1.4 MeV in excitation in ^{99}Nb. Their calculations would predict population of this state, since in

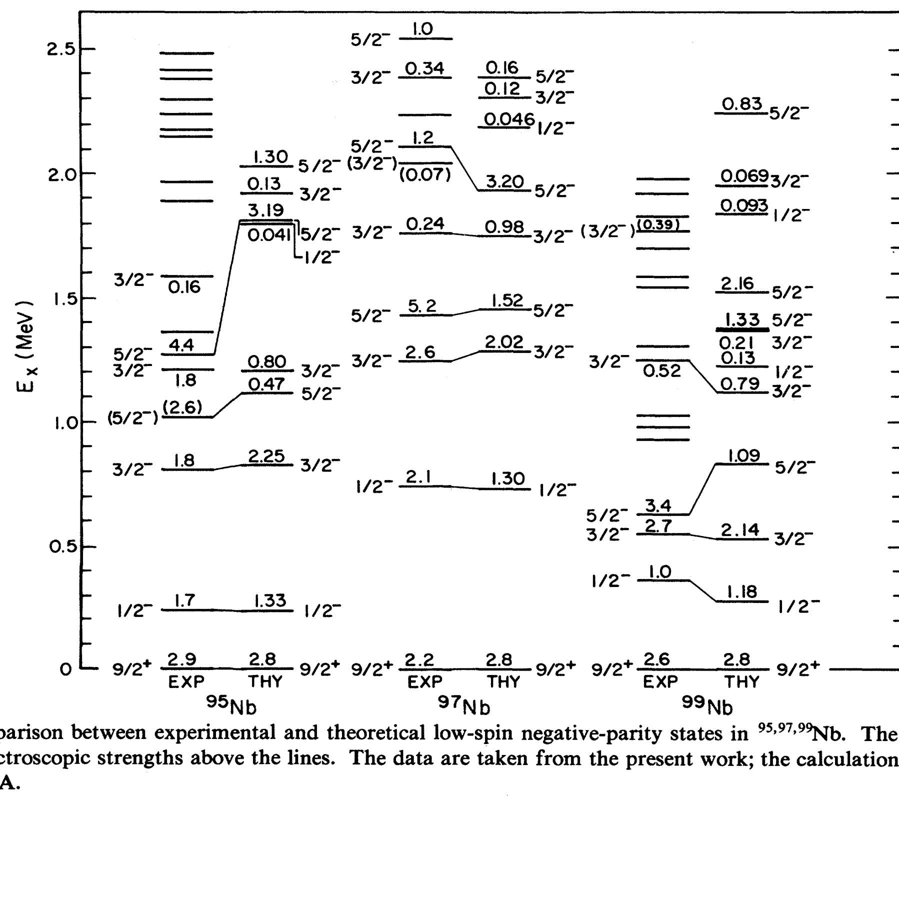

FIG. 10. Comparison between experimental and theoretical low-spin negative-parity states in ^{95,97,99}Nb. The levels are labeled by J^π values and spectroscopic strengths above the lines. The data are taken from the present work; the calculations are from Ref. 9 using parameter set A.

their model it is an equal admixture of the $d_{5/2}$ and $g_{9/2}\otimes 2_1^+$ configurations. Other positive-parity states would not be populated, since they are predominantly $g_{9/2}\otimes 2_1^+$ configurations, which is not in agreement with the observations of excited $\frac{9}{2}^+$ and, possibly, $\frac{7}{2}^+$ states in the Nb nuclei via our present $(\vec{t},\alpha)$ measurements.

Given the overall agreement between the empirical spectroscopic information on the Nb isotopes and the relatively simple core-coupling calculations of Ref. 9, the trend towards deformation in the Nb nuclei does not seem more rapid than in the Mo nuclei. This is in contrast to Zr where an abrupt change in structure is observed between $N=58$ and 60.

VI. CONCLUSIONS

The $(\vec{t},\alpha)$ study of the Mo isotopes and of ^{96}Zr has produced a large number of new definitive spin assignments and a number of new energy levels. The results confirm a previous suggestion of the ground state configuration of ^{96}Zr. They also indicate that the $N=56$ subshell closure has an appreciable effect on the Nb isotopes. This, however, is contrasted with the apparently slow onset of a tendency towards deformation which is more like the Mo nuclei than the Zr nuclei.

[1]E. Chiefetz, R. C. Jared, S. G. Thompson, and J. B. Wilhelmy, Phys. Rev. Lett. 25, 38 (1970).

[2]K. Sistemich, W. D. Lauppe, H. Lawin, H. Seyforth, and B. D. Kern, Z. Phys. A 289, 225 (1979).

[3]K. Sistemich, G. Sadler, T. A. Khan, H. Lawin, W. D. Lauppe, H. A. Seliie, F. Schussler, J. Blachot, E. Monnand, J. P. Bocquet, and B. Pfeiffer, Z. Phys. 281, 169 (1977).

[4]R. F. Casten, E. R. Flynn, O. Hansen, and T. J. Mulligan, Nucl. Phys. A184, 357 (1972).

[5]E. R. Flynn, F. Ajzenberg-Selove, R. E. Brown, J. A. Cizewski, and J. W. Sunier, Phys. Rev. C 24, 2475 (1981).

[6]H. Taketani, M. Adachi, M. Ogawe, K. Ashibe, and T. Hattari, Phys. Rev. Lett. 27, 520 (1971).

[7]P. Van Isacker and G. Puddu, Nucl. Phys. A348, 125 (1980); M. Sambataro and G. Molnar, *ibid.* A376, 201 (1982).

[8]P. Federman and S. Pittel, Phys. Rev. C 20, 820 (1979).

[9]P. K. Bindal, D. H. Youngblood, and R. L. Kozub, Phys. Rev. C 10, 729 (1974); P. K. Bindal and D. H. Youngblood, *ibid.* 9, 1618 (1974).

[10]B. M. Preedom, E. Newman, and J. G. Hiebert, Phys. Rev. 166, 1156 (1969).

[11]L. R. Medsker and J. L. Yntema, Phys. Rev. C 7, 440 (1973); L. R. Medsker, *ibid.* 8, 1906 (1973).

[12]E. R. Flynn, F. Ajzenberg-Selove, R. E. Brown, J. A. Cizewski, and J. W. Sunier, Phys. Rev. C 24, 902 (1981).

[13]R. A. Hardekopf, in *Proceedings of the Fourth International Symposium on Polarization Phenomena in Nuclear Reactions,* edited by W. Grüebler and V. König (Birkhäuser, Basel, 1976), p. 865.

[14]S. D. Orbesen, J. D. Sherman, and E. R. Flynn, Los Alamos Scientific Laboratory Report LA-6271-MS, 1975.

[15]*Tables of Isotopes,* 7th ed., edited by C. M. Lederer and V. Shirley (Wiley, New York, 1978).

[16]A. H. Wapstra and K. Bos, At. Data Nucl. Data Tables 19, 175 (1977).

[17]P. D. Kunz, University of Colorado report (unpublished).

[18]E. R. Flynn, D. D. Armstrong, J. G. Beery, and A. G. Blair, Phys. Rev. 182, 1113 (1969).

[19]K. Matsuda, Y. Awaya, H. Nakanishi, and S. Takeda, J. Phys. Soc. Jpn. 33, 298 (1972).

[20]B. M. Preedom, E. R. Flynn, and N. Stein, Phys. Rev. C 11, 1691 (1975).

[21]E. R. Flynn, J. G. Beery, and A. G. Blair, Nucl. Phys. A218, 285 (1974).